



**HAL**  
open science

# Ultra-broadband continuum generation in silica based defective core photonic crystal fiber

A. Sharafali, K. Nithyanandan

► **To cite this version:**

A. Sharafali, K. Nithyanandan. Ultra-broadband continuum generation in silica based defective core photonic crystal fiber. *Optik*, 2019, 191, pp.121 - 131. 10.1016/j.ijleo.2019.06.014 . hal-03484512

**HAL Id: hal-03484512**

**<https://hal.science/hal-03484512>**

Submitted on 20 Dec 2021

**HAL** is a multi-disciplinary open access archive for the deposit and dissemination of scientific research documents, whether they are published or not. The documents may come from teaching and research institutions in France or abroad, or from public or private research centers.

L'archive ouverte pluridisciplinaire **HAL**, est destinée au dépôt et à la diffusion de documents scientifiques de niveau recherche, publiés ou non, émanant des établissements d'enseignement et de recherche français ou étrangers, des laboratoires publics ou privés.



Distributed under a Creative Commons Attribution - NonCommercial 4.0 International License

# Ultra-broadband continuum generation in silica based defective core photonic crystal fiber

Sharafali.A<sup>a</sup>, K. Nithyanandan<sup>b,\*</sup>

<sup>a</sup>Department of Physics, Pondicherry University, Puducherry, India 605014

<sup>b</sup>CNRS/Universite Joseph Fourier, Laboratoire Interdisciplinaire de Physique (LIPHY), 38402 Saint-Martin-d'Hères, Grenoble, France.

---

## Abstract

We investigate a defective core photonic crystal fiber for broadband continuum generation. Different geometries of fiber design are discussed to emphasize the role of a defect in the fiber characteristics. The idea of incorporating a defect in the core enable an additional degree of design freedom to tailor the fiber parameters. Particularly, we identify that by properly choosing the size of the defect and air hole size one can realize suitable fiber design for various nonlinear applications. Out of several fiber designs, we recognize that designing fiber with minimum positive dispersion along with a large nonlinearity coefficient is a potential candidate for supercontinuum generation. The results of numerical simulation of the broadband continuum at different parameter settings are analyzed and compared with the conventional counterpart. In the similar simulation environment, the continuum realized in the proposed defective core photonic crystal fiber is significantly broader than the fiber without defect. Thus, this hybrid fiber design can be a new class of fibers for the future generation of broadband sources.

---

## 1. Introduction

An elegant control of fiber parameters through robust engineering techniques made the photonic crystal fiber (PCF) as the medium of choice for a wide range of applications [1, 2, 3, 4, 5, 6]. Starting from the core research led by Russell's group in the late 1990s, the research in PCF finds different varieties of geometrical structures made out of different materials [6, 7, 8, 9, 10, 11]. The two major class of photonic crystal fibers are the solid core PCF and hollow core photonic PCF. Even though the hollow core PCF with band gap guidance mechanisms can be used for different applications, filling different novel materials in the central hole, make it useful for many nonlinearity based applications under the principle of index guidance mechanism as in solid core PCF [6, 7, 8, 9, 10, 11]. Unlike conventional step-index fibers, PCFs are made by using a number of silica-based cylindrical capillaries arranged in a predefined lattice format. The diameter of each capillary and the separation of them from each neighbour, referred to as pitch, defines the fiber properties like dispersion and nonlinearity coefficients, etc. Further enhancement in fiber properties can be made by means hybrid design such as tapering the fiber along the fiber length or altering the fiber materials, to mention a few (refer papers [12, 13, 14, 15, 33], and the references therein). In the last two decades, different techniques have been proposed and implemented to enhance the nonlinear property of the fiber for various nonlinear applications. One of such recent techniques to enhance the nonlinearity of the fiber is through defective core PCF (DCPCF) [17, 18, 19, 20]. In this model, a sub-wavelength defect at the center of the core region

reduces the effective area of the fiber and thereby enhances the nonlinearity of the fiber. Such fibers can be used for applications requiring high nonlinearity like supercontinuum generation (SCG).

As a potential alternate to *white-light laser*, PCF based SCG became an active area of research in optical technologies [1, 2, 3, 4, 21, 22, 23, 24, 25]. It also finds applications in generation of ultra-short pulses, frequency metrology, optical coherence tomography (OCT) systems etc [26, 27, 28]. An ultra-broad continuum generation by passing an intense light beam through a nonlinear medium is extensively studied by different research groups both theoretically and experimentally [29, 30, 31, 32, 33, 34, 35, 36, 37, 38, 39, 40, 41, 42]. The process governing the SCG can be triggered by two mechanisms namely modulation instability and soliton fission [1, 2, 3, 4, 21, 22, 23, 24, 25, 29, 30, 31, 32, 33, 30, 43, 44, 45]. It is also very evident that the continuum generated critically depends on the pulse parameters such as input power, width as well as the fiber parameters like nonlinearity, dispersion and loss, etc., Hence designing fiber with appropriate dispersion and nonlinear profile is a crucial part in the broadband generation.

Recently, F. Li *et. al* reported highly coherent and broad continuum generation in a solid core photonic crystal fiber by passing a self-similarly compressed pulse through a non-zero dispersion shifted fiber (NZ-DSF) [46]. The self-similar pulse compression is achieved in a tapered large mode area fiber exhibiting very high nonlinearity. Using a highly compressed pulse results in increasing the spectral width of the continuum generated along with high coherence. Another model known as suspension core PCF was used to enhance the continuum width through an increase in nonlinearity coefficient by decreasing the effective area. In this model, the first layer of the air hole capillaries is suspended towards the core regime to reduce the effective core area [47]. Another method to enhance the

---

\*Corresponding author  
Email addresses: sharaf.saj@gmail.com (Sharafali.A),  
nithi.physics@gmail.com (K. Nithyanandan)

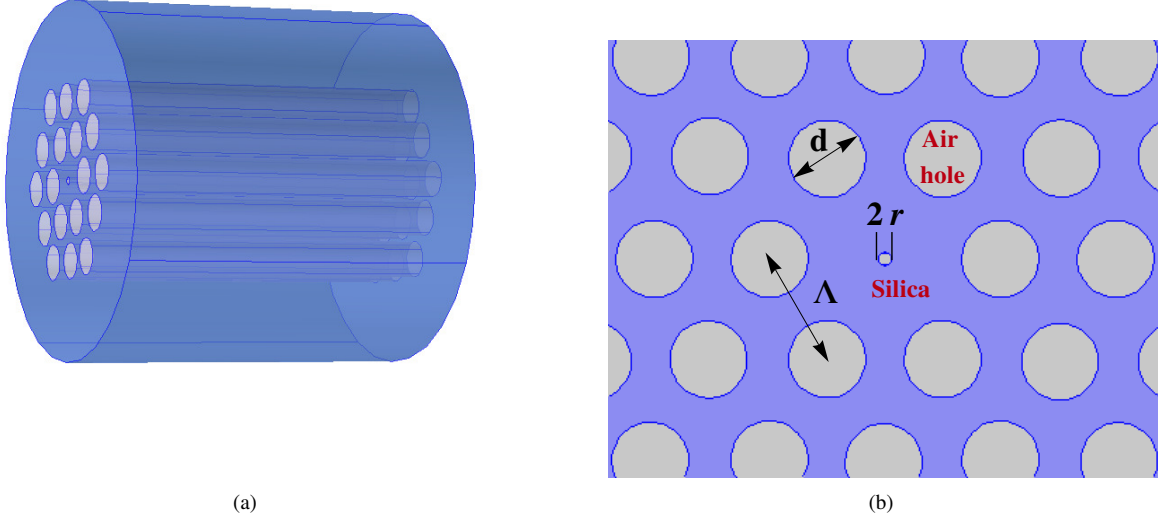


Figure 1: (Color online) (a) Longitudinal and (b) cross sectional view of the defective core PCF

spectral width is through non-silica technology by infiltrating nonlinear liquids such as carbon tetrachloride, carbon disulphide etc. in the fiber core regime [48, 49, 50, 51]. The high nonlinear refractive index of these nonlinear liquids provides high nonlinearity coefficients than that of silica-based fibers. However, one of the major challenges in those design is the high loss encountered by the PCF after infiltration. Also, the safety limit and toxicity level of those nonlinear liquids become a major constraint for practical application. Besides all, in this paper, we have modeled silica-based defective core PCFs, which when properly designed is capable of simultaneous enhancement of nonlinearity along with minimum positive dispersion coefficient. This combination of dispersion and nonlinear profile is identified to be the suitable candidate for nonlinear applications especially SCG.

The organization of the paper is as follows: After the introduction, Sec. 2 describes the design of the proposed DCPCF and the calculation of fiber parameters. Sec. 3 explains theoretical modeling and simulation results of SCG. Discussion of the results is part of Sec. 4, while Sec. 5 concludes the paper with a brief summary of the results.

## 2. DESIGNING THE DEFECTIVE CORE PHOTONIC CRYSTAL FIBER

The characteristics of PCF are very much dependent on the choice of the fiber as well as on the geometry of the microstructure lattice. Hence designing fiber for specialized application is a very crucial part in PCF enabled photonic technologies. Besides, the fiber parameters like dispersion and nonlinearity coefficients are very much dependent on the diameter of the air hole capillaries and the pitch of the fiber. This enables

one to easily maneuver the characteristics of fiber by controlling these parameters. In the present context, we have used the commercial simulation software COMSOL 5.2a to design the fiber geometry and the mode analysis has been performed by finite element method (FEM). A hexagonal lattice of  $\Lambda=1.8\mu\text{m}$  with different air hole diameters and defective core radius are considered as shown in Fig. (1). In realistic situations, these can be controlled by proper management of drawing speed, furnace temperature, etc. A longitudinal variation in pitch and air hole diameter along the fiber length can also be fulfilled by tapering technique. A circular phase matched layer was used to nullify the backscattered radiation from the boundaries of simulation area [52]. The effective refractive index has been calculated through mode analysis by using the linear refractive index of silica as follows [53],

$$n_{\text{silica}} = \frac{(0.788404+23.5835 \times 10^{-6}T) \times \lambda^2}{\lambda^2 - (0.0110199+0.584758 \times 10^{-6}T)} + 1.31552 + 6090754 \times 10^{-6}T + ((0.91316 + 0.548368 \times 10^{-6}T) \times \lambda^2) / \lambda^2 - 100. \quad (1)$$

The dispersion and nonlinearity coefficient corresponding to each fiber are evaluated by using the expression,

$$D(\lambda) = -\frac{\lambda}{c} \frac{d^2 n_{\text{eff}}}{d\lambda^2} \quad (2)$$

$$\gamma = \frac{2\pi n_2}{\lambda A_{\text{eff}}} \quad (3)$$

$$A_{\text{eff}} = \frac{(\int \int |E|^2 dx dy)^2}{\int \int |E|^4 dx dy}. \quad (4)$$

where  $\gamma$  stands for nonlinearity coefficient,  $n_{\text{eff}}$  represents the effective refractive index,  $\lambda$  is the wavelength,  $A_{\text{eff}}$  is the

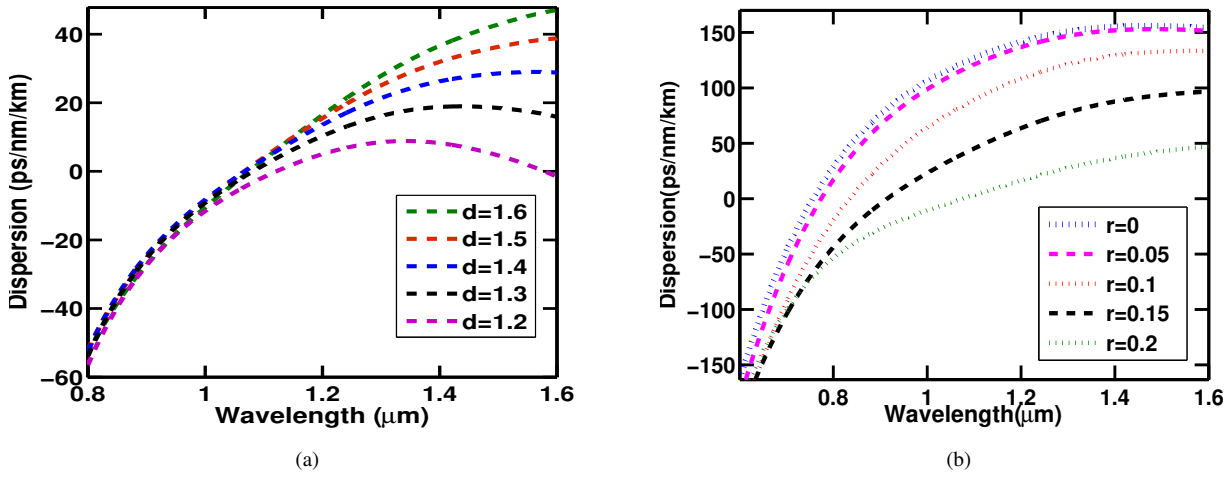


Figure 2: (Color online) Variation of dispersion with wavelength for (a) different air hole diameter at  $r=0.2\mu\text{m}$  (b) and defect radius at  $d=1.6\mu\text{m}$ .

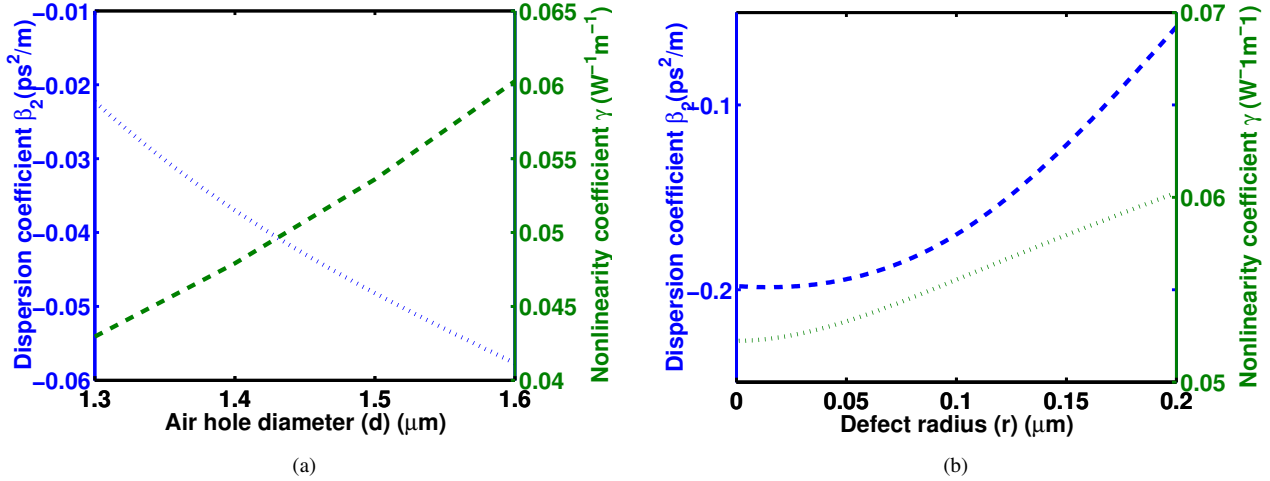


Figure 3: (Color online) Variation of dispersion and nonlinearity coefficient with (a) different air hole diameter at  $r=0.2\mu\text{m}$  (b) and defect radius at  $d=1.6\mu\text{m}$  at  $\lambda=1550\text{ nm}$ .

effective area and  $n_2$  stands for nonlinear refractive index [53].

The dispersion variation with wavelength for all the proposed PCF geometries are depicted in Fig. (2). Note, the dispersion here is actually the dispersion parameter represented typically by  $D$  in units of ps/nm/km and this should not be confused with the dispersion coefficient  $\beta_2$  in units of ps<sup>2</sup>/km. One can observe from Fig. (2) that the dispersion ( $D$ ) shifts from normal to anomalous dispersion regime as the wavelength increases. The recorded zero dispersion wavelength (ZDW) clearly indicates the dependence of ZDW on the size of the air hole and defect. At the operating wavelength  $\lambda=1550\text{ nm}$ , the dispersion shifts towards zero dispersion point if  $d$  decreases for a fixed  $r$  or vice-versa (Refer. Fig. 2 (a) and (b)).

The dispersion variation can be better understood while inspecting the variation of second order dispersion coefficient

with  $d$  and  $r$  values at  $\lambda=1550\text{ nm}$ . It is evident from Fig. 3(a) and (b) that increasing  $d$  for getting high nonlinearity is not an appropriate choice as it also tends to increase the dispersion coefficient. On further examination of Fig. 3(a) and (b) reveals the possibilities for the enhancement of the nonlinearity coefficient by increasing defective air hole radius and the diameter of air hole capillaries. For better understanding, the parameters obtained for the different combinations of fiber design are tabulated in Tab 1. As it can be seen from the evaluated numerical data, the defect in the core regime can lead to an increase in nonlinearity coefficient by reducing the effective area of the fiber for a fixed air hole diameter value. A shift in dispersion coefficient (nonlinearity coefficient) from  $-0.1982\text{ ps}^2/\text{m}$  ( $0.0522\text{ W}^{-1}\text{m}^{-1}$ ) to  $-0.0577\text{ ps}^2/\text{m}$  ( $0.0602\text{ W}^{-1}\text{m}^{-1}$ ) is recorded by incorporating a defective air hole of radius  $0.2\text{ }\mu\text{m}$ . This particular property of enhanced

nonlinearity coefficient accompanied by minimum positive dispersion in the proximity of zero dispersion is an ideal scenario for efficient phase matching condition for the nonlinear process such as supercontinuum generation.

We have also calculated the confinement loss ( $\alpha$ ) and confinement factor (in %) ( $\Gamma$ ) of all different PCF geometries of choice by using the following formulae [56, 55],

$$\alpha = 8.686 \frac{2\pi}{\lambda} \text{Im}(n_{eff}) \text{ dB/m} \quad (5)$$

$$\Gamma = \frac{\int_i |E(x, y)|^2 dx dy}{\int_{-\infty}^{\infty} |E(x, y)|^2 dx dy} \times 100. \quad (6)$$

The variation of confinement loss and confinement factor are depicted in Fig. (4). From the confinement factor and loss analysis, we can observe that the field is better confined in the core regime for increased air hole diameter values for a fixed defective air hole radius. This is due to the decrease in the effective index of cladding with an increase in the air-filling fraction. Due to this high confinement for large  $d$  values, the leakage through cladding will be less and the fiber tends to become multimode. In order to find the mode of operation, we have calculated the  $V$  parameters of the PCFs proposed by using the expression [57],

$$V_{PCF} = \frac{2\pi\Lambda}{\lambda} \sqrt{n_{FM}(\lambda)^2 - n_{FSM}(\lambda)^2} \quad (7)$$

Where  $n_{FM}(\lambda)$  and  $n_{FSM}(\lambda)$  are the effective index of the fundamental mode and fundamental space filling mode. The threshold for the single mode operation is given by  $V_{PCF}=\pi$ . This has been theoretically formulated by M. D. Nielsen *et. al.* and later verified experimentally [58]. The  $V_{PCF}$  parameters of the designed PCFs with different  $d$  and  $r$  values is shown in Fig. (5). It can be noticed that  $V_{PCF}$  is increasing with air hole diameter whereas it goes down while increasing the defective air hole size. An effective single mode operation can be made possible by choosing DCPCF with small  $d$  and large  $r$  parameters. Conventional means of decreasing the air hole size to reduce the  $V$  parameter to achieve the single mode operation with a fixed pitch is rather limited because it tends to decrease nonlinearity. Thus the incorporation of the defective core in PCF enables additional degrees of freedom to tailor the system characteristics best suitable for nonlinear applications, (*i.e.*), enhanced nonlinearity with minimum positive dispersion within the single mode operation. For this, we have identified a DCPCF with  $d=1.2\mu\text{m}$  and  $r=0.2\mu\text{m}$  as the best candidate which gives  $V_{PCF}=2.122$  and thus ensures a single mode operation at  $\lambda_p=1550\text{ nm}$ . The dispersion and nonlinearity coefficients variation of PCF designed under this parametric condition are tabulated in Tab II.

### 3. Supercontinuum generation

The equation governing the propagation of an ultrashort optical pulse in PCF is given by the generalized nonlinear Schrödinger equation (GNLSE) of the form as follows [1, 2]

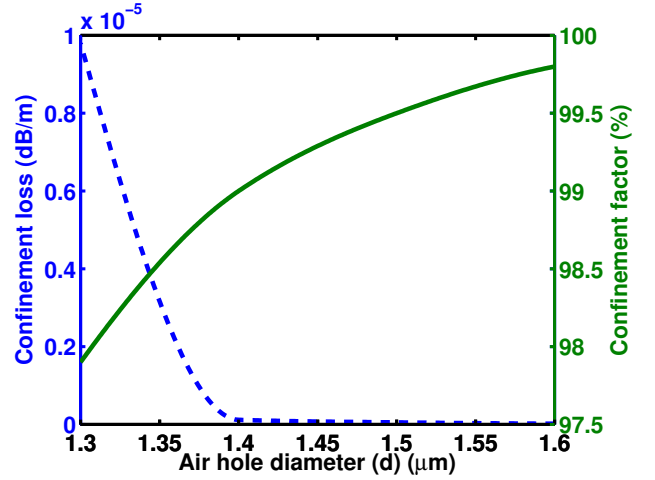


Figure 4: (Color online) Confinement loss and confinement factor variation of DCPCFs with different air hole diameter at  $r=0.2\mu\text{m}$  considered.

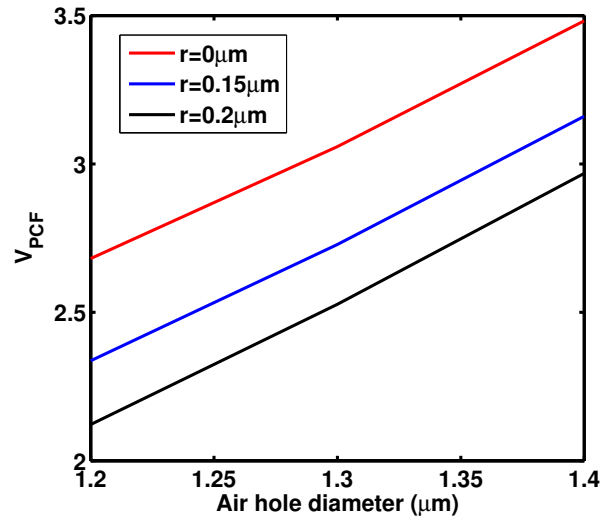


Figure 5: (Color online)  $V_{PCF}$  parameter variation of DCPCFs having different  $d$  and  $r$  values.

Air hole diameter $d=1.6\mu\text{m}$			
Parameters	$r=0\ \mu\text{m}$	$r=0.1\ \mu\text{m}$	$r=0.2\ \mu\text{m}$
$\beta_2$ (ps <sup>2</sup> /m)	-0.1982	-0.1701	-0.0577
$\beta_3$ (ps <sup>3</sup> /m)	$4.433\times 10^{-5}$	$4.324\times 10^{-5}$	$2.473\times 10^{-5}$
$\beta_4$ (ps <sup>4</sup> /m)	$-9.317\times 10^{-9}$	$-8.442\times 10^{-9}$	$-3.577\times 10^{-9}$
$\gamma$ (W <sup>-1</sup> m <sup>-1</sup> )	0.0522	0.0555	0.0602
Defective core radius $r=0.2\ \mu\text{m}$			
Parameters	$d=1.4\ \mu\text{m}$	$d=1.5\ \mu\text{m}$	$d=1.6\ \mu\text{m}$
$\beta_2$ (ps <sup>2</sup> /m)	-0.0371	-0.0482	-0.05772
$\beta_3$ (ps <sup>3</sup> /m)	$9.871\times 10^{-6}$	$1.807\times 10^{-5}$	$2.473\times 10^{-5}$
$\beta_4$ (ps <sup>4</sup> /m)	$-8.166\times 10^{-9}$	$-5.017\times 10^{-9}$	$-3.577\times 10^{-9}$
$\gamma$ (W <sup>-1</sup> m <sup>-1</sup> )	0.0479	0.0535	0.0602

Table 1: Variation of dispersion and nonlinearity coefficients with  $d$  and  $r$  for the different PCF geometries.

Air hole diameter $d=1.2\mu\text{m}$					
Parameters	$r=0\ \mu\text{m}$	$r=0.05\ \mu\text{m}$	$r=0.1\ \mu\text{m}$	$r=0.15\ \mu\text{m}$	$r=0.2\ \mu\text{m}$
$\beta_2$ (ps <sup>2</sup> /m)	-0.1172	-0.1079	-0.08681	-0.0542	-0.0029
$\beta_3$ (ps <sup>3</sup> /m)	$1.5228\times 10^{-5}$	$1.305\times 10^{-5}$	$1.045\times 10^{-5}$	$7.6711\times 10^{-6}$	$4.3736\times 10^{-6}$
$\beta_4$ (ps <sup>4</sup> /m)	$-1.061\times 10^{-9}$	$-1.803\times 10^{-9}$	$-2.442\times 10^{-9}$	$-2.933\times 10^{-9}$	$-3.319\times 10^{-9}$
$\gamma$ (W <sup>-1</sup> m <sup>-1</sup> )	0.0345	0.0351	0.0363	0.0375	0.0383
$V_{PCF}$	2.681	2.631	2.5064	2.337	2.122

Table 2: Variation of fiber parameters for different size of defect in DCPCF with  $d=1.2\mu\text{m}$ .

$$\frac{\partial U}{\partial z} + \sum_{n=2}^4 \beta_n \frac{i^{n-1}}{n!} \frac{\partial^n U}{\partial t^n} + \frac{\alpha}{2} U = i\gamma \left( 1 + i\tau_{shock} \frac{\partial}{\partial t} \right) \times \left( U(z, t) \int_{-\infty}^{\infty} R(t') |U(z, t-t')|^2 dt' \right) \quad (8)$$

where  $U(z, t)$  represents the electric field amplitude,  $z$  and  $t$  are the longitudinal coordinate and time in the moving reference frame, respectively. The dispersion coefficient  $\beta_n$  attributes to the Taylor expansion of the propagation constant around the center frequency  $\omega_0$  and  $n$  being the order of dispersion.  $\gamma$  and  $\alpha$  respectively amounts to the fiber nonlinearity and losses. The time derivative term on the right-hand side of Eq. (8) takes into account the dispersion of the nonlinearity, which is usually associated with the optical shock formation. The typical characteristic timescale of the shock is given by  $t_{shock} = 1/\omega_0$ .  $R(t)$  is the response function which takes into account both the instantaneous electronic response and the delayed Raman response. The functional form of  $R(t)$  can be written as [59, 60, 61, 62, 63]

$$R(t) = (1 - f_R)\delta(t) + f_R h_R(t) \quad (9)$$

where  $h_R$  is the retarded response function and  $f_R$  amounts to fractional contribution to the delayed Raman response.  $\delta(t)$  is the Dirac delta function. The functional form of the retarded

function ( $h_R$ ) can be given as

$$h_R = \frac{\tau_1^2 + \tau_2^2}{\tau_1 \tau_2^2} \sin\left(\frac{t}{\tau_1}\right) e^{-\frac{t}{\tau_2}} \Theta(t) \quad (10)$$

with  $f_R=0.18$ ,  $\tau_1 = 0.012$  ps, and  $\tau_2 = 0.032$  ps [59, 60, 61, 62, 63].  $\Theta(t)$  is the heavyside step function.

To investigate the propagation dynamics and SCG, we numerically solved Eq. (8) using split-step Fourier method (SSFM) with the input profile of the form  $U(0, t) = N \text{sech}(t/\tau_0)$ , where  $N$  is the soliton order determined by the system parameters that includes both the pulse as well as the fiber parameters [2, 59]. Numerical simulations are carried out using a 0.1 ps duration soliton-like pulse with a peak power of 1 kW at pump wavelength  $\lambda_p=1550$  nm. The fiber parameters used for simulations are listed in Tab. II.

In the anomalous dispersion regime pumping, the spectral broadening leading to supercontinuum is typically governed by the soliton-driven dynamics. In the parametric space of our choice, the so-called soliton fission (SF) being the most important stage in the spectral broadening process, such that, the initial pulse profile set by the system parameters constitute a higher-order soliton which on perturbation breaks up into  $N$  soliton-like pulses. Depending on the combination of system parameters, the initial input profile changes, which substantially influence the spectral and temporal evolution which can be obvious from the subsequent discussion. To highlight the effect of

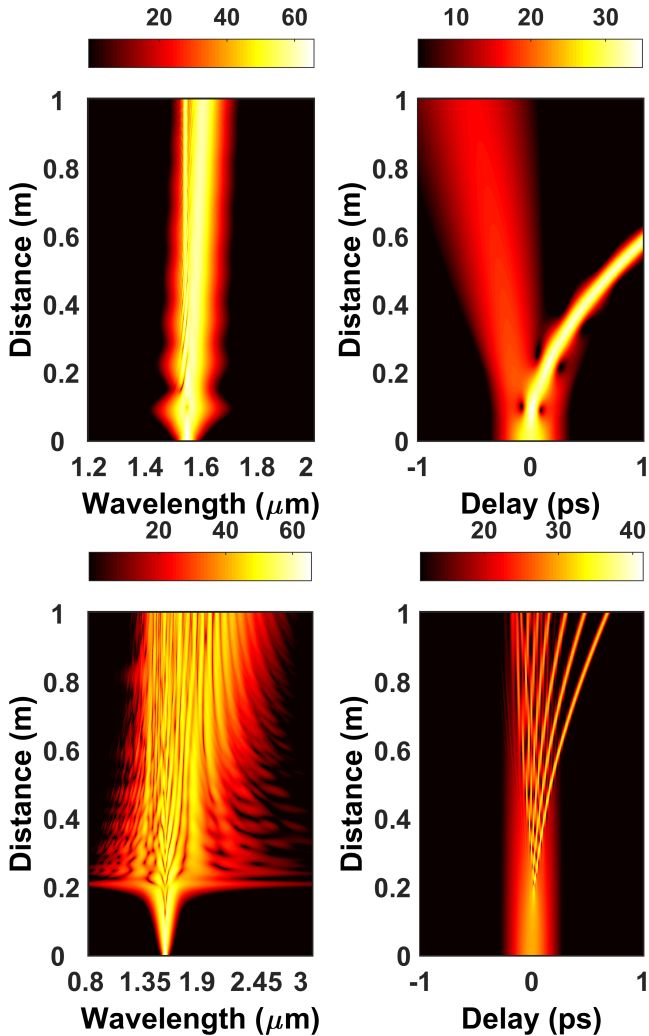


Figure 6: (Color online) Spectral and temporal evolution of in PCF with and without defect. Top panel is PCF  $d=1.2\mu\text{m}$ ,  $r=0\mu\text{m}$ , while bottom panel corresponds to DCPCF with  $d=1.2\mu\text{m}$ ,  $r=0.2\mu\text{m}$ .

a defect in the SCG, we show in the Fig. (6) the spectral and the temporal evolution of pulse propagation in two representative cases of PCF with and without defect. The fiber parameters are given in the caption, and the corresponding system parameters can be inferred from Tab. II.

In similar lines to the earlier discussion on SCG, the initial stage of propagation is governed by a symmetrical spectral broadening, resulting from the temporal compression of the propagating higher-order soliton. Further propagation down the fiber, when subjected to perturbation brings the soliton fission into the picture. The distance of the onset of the soliton fission is characteristic of the system which is set by its parameters. In principle, the injected higher-order soliton tends to split when its bandwidth reaches a maximum. In the present parametric space, both the higher order dispersion and Raman scattering accounts to perturbation and thereby contribute to fission of solitons. The constituent soliton resulting from the fission experiences a continuous shift due to soliton self-frequency resulting

from Raman scattering [64, 65, 66]. Owing to the difference in the initial profile (or soliton order) of the higher-order soliton as a result of reduced dispersion and increased nonlinearity in the case of DCPCF, the corresponding spectral evolution significantly differs from the case of fiber without defect as it is shown in Fig. (6). In both cases, an obvious continuous red-shift of the long wavelength components is apparent, confirming the strong influence of the soliton self-frequency shift. In addition to the spectral extension on the long wavelength side, a narrow band resonance on the normal group velocity dispersion regime can be noticed, which is identified as the dispersive wave generation (DWG). The higher-order dispersion accounts for the DWG, whose position is determined by the phase matching condition. It is apparent from the Fig. (6) the bandwidth of the continuum generated by DCPCF is broader, which is attributed to the increase in soliton-order resulting from the reduced dispersion and the increased nonlinearity.

#### 4. Results and Discussion

For a comprehensive understanding on the role of the defect in the spectral evolution, we show respectively in Fig. (7) and (8), the spectral and the temporal evolution in 1 m long DCPCF with different defect size in step of  $0.05\mu\text{m}$ . It is obvious that an increase in the defect size invariably broadens the spectrum as shown in Fig. (7). This is attributed to the increase in the soliton order as a result of the reduced dispersion and increased nonlinearity. As the relation connecting the soliton order ( $N$ ) with dispersion length ( $L_D$ ) and nonlinear length ( $L_{NL}$ ) is apparent  $N = \sqrt{L_D/L_{NL}}$ , one can straightforwardly understand that the incorporation of defect naturally tends to increase the soliton order. As the soliton order and fission length are connected through the dispersion length given by  $L_{fis} = L_D/N$ , the fiber design that supports increased nonlinearity with minimum positive dispersion is the appropriate condition to increase the soliton order for fixed pulse parameters. Thus, 1m long DCPCF when pumped by a 0.1 ps soliton at a constant pump power of 1 kW evolves as a higher-order soliton of order  $N$  depending on the size of the defect. As the soliton order depends on both the pulse and fiber parameters, when the size of the defect increases the dispersion decreases while the nonlinearity increases as shown in the Fig. (2) and (3), respectively. This variation of dispersion and nonlinearity increase the soliton order and thereby assist the spectral broadening.

It should be noted that the short wavelength edge of the spectrum set by the DWG does not see much of changes from case to case, while the major spectral broadening is attributed to the long wavelength extension as a result of the soliton self-frequency shift. Temporal evolution perhaps gives a clear signature of the soliton fission and the evolution of the ejected lower amplitude soliton pulses. Fig. (7) implies in-common that it is only the Raman soliton self-frequency shift is responsible for the long wavelength extension and thus crucial in determining the overall bandwidth of the spectrum. It is apparent that the defect increases the bandwidth of the continuum, however, the role of the defect in the spectral broadening is only obvious on

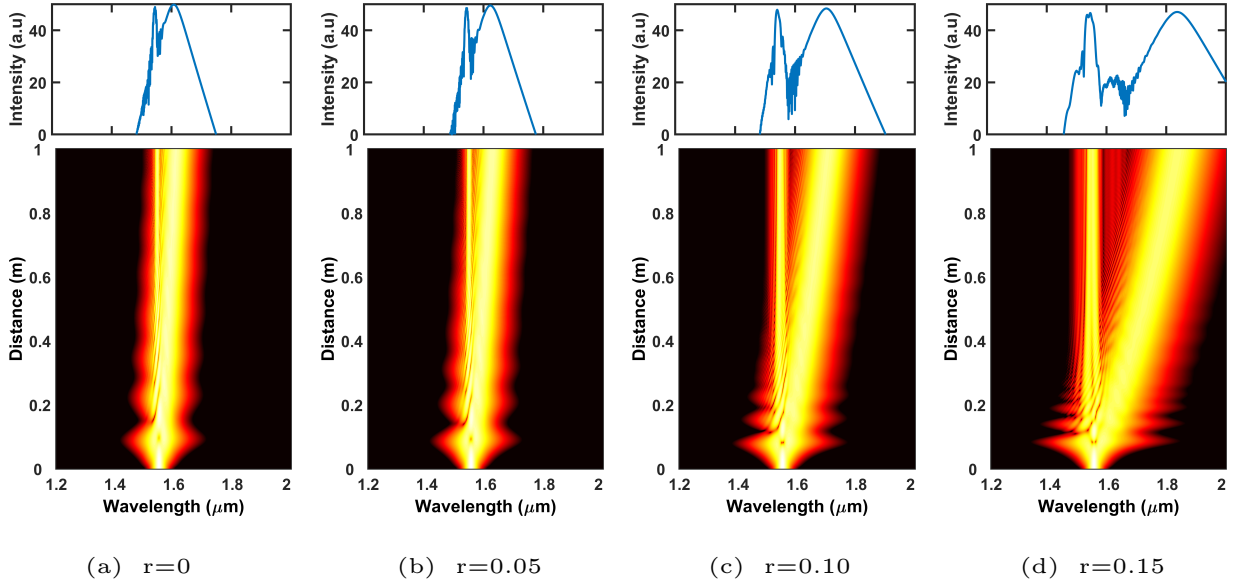


Figure 7: (Color online) Spectral evolution in DCPCF for different defect size. The top panel represents the output spectrum, while the bottom panel is the density plot representation of the spectral evolution as a function of distance.

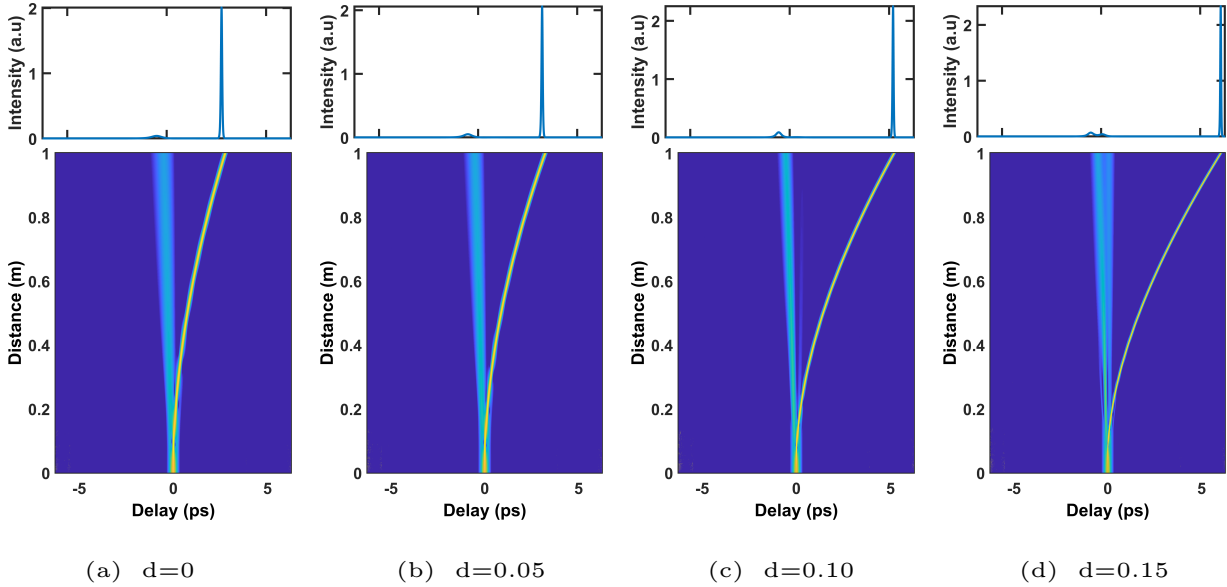


Figure 8: (Color online) Temporal evolution in DCPCF for different defect size. The top panel represents the output field intensity, while the bottom panel is the time-domain density representation of the field intensity as a function of distance.

Characteristics of Raman self-frequency shift				
Parameters	$r=0 \mu\text{m}$	$r=0.05 \mu\text{m}$	$r=0.1 \mu\text{m}$	$r=0.15 \mu\text{m}$
Shift (ps)	2.761	3.233	5.188	6.035
Width (fs)	71.72	68.67	56.46	47.30
Intensity (a.u)	2.01	2.059	2.229	2.302

Table 3: Characteristics of Raman soliton self-frequency shift for DCPCF with  $d=1.2\mu\text{m}$  for different defect radius.

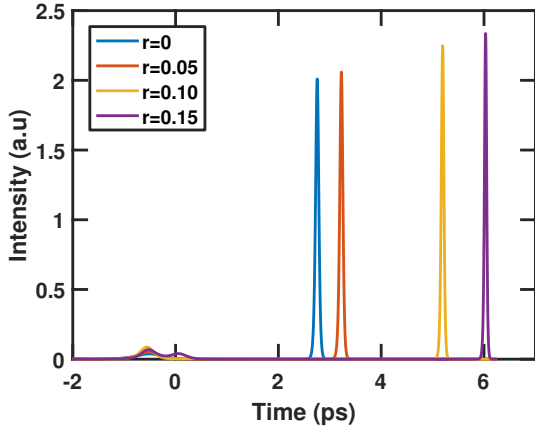


Figure 9: (Color online) Time domain representation of output intensity after a propagation of 1m in DCPCF for different size of defect.

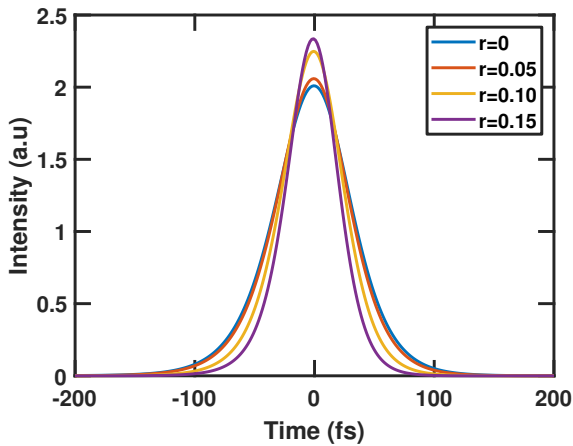


Figure 10: (Color online) Expanded view of the Raman soliton corresponding to different defect size.

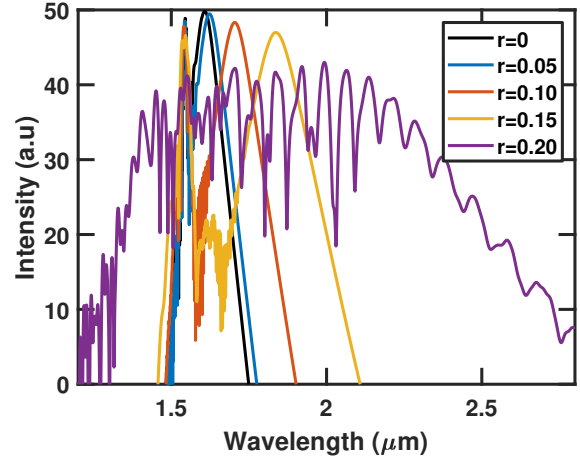


Figure 11: (Color online) Supercontinuum spectrum in 1m of DCPCF for different size of defect.

careful examination of the temporal evolution of Raman soliton as shown in Fig. (8). The evolution of the Raman soliton and the associated spectral broadening can be best explained by the theory of soliton fission. The higher order soliton undergoing fission ejects soliton in an orderly fashion such that the soliton with highest peak power undergoes maximum drift due to relatively higher group velocity difference with that of the pump wavelength. In other words, the soliton with the highest amplitude exhibits the shortest width and travel faster during propagation. As it is evident from the theory of soliton fission, the width of the ejected soliton exhibit an inverse relation with soliton order, such that, an increase in the soliton order results in the emission of Raman soliton with high peak power and reduced width, which can be evident on the careful examination of temporal evolution of Raman soliton for different core size. This has been a crucial point in the whole discussion. For better insight, we show in Fig. (9), the recorded temporal intensity profile at the output of 1 m length of DCPCF for some representative values of defect size. It is straightforward to notice from Fig. (9), the downshift of the Raman soliton increases with increase in the size of the defect (refer Tab.III). This preponderance is attributed to the fact that the higher amplitude soliton (or short soliton) experience relatively greater self-frequency shifts and rapidly walk-off from the pump wavelength as it is obvious from Fig. (9).

Additional insight on the effect of defect size on the Raman soliton can be evident from the expanded view of the Raman

soliton shown in Fig. (10). It is apparent that when the size of the defect increases, the width (amplitude) of the ejected soliton reduces (increases) as a consequence of the increase in soliton order. We use the  $\text{sech}^2$  fit to evaluate the width of the Raman soliton and the estimated width shows a monotonous decrease with increase in the defect size (refer Tab.III). This decrease in the soliton width tends to broaden the spectrum as a result of the increased overlap of the soliton bandwidth with the Raman gain (refer Fig. 7 and corresponding time-domain representation in Fig. 8). For a comprehensive picture, we show in Fig. (11), the supercontinuum spectrum in the 1 m long DCPCF for different defect size. It is evident that the spectral width of continuum produced by the DCPCF is much broader than that of conventional solid core PCF and further broadening can be achieved by proper choice of the defect size. For numerical appreciation, we demonstrate a broadband spectrum spanning more than an octave in 1 m of DCPCF with a defect size of  $r=0.2\mu\text{m}$  (refer Fig. 11).

## 5. Conclusion

In summary, we demonstrate a broadband continuum in a photonic crystal fiber with a sub-wavelength defect. The incorporation of a defect in the core enables an additional degree of design freedom to tailor the characteristic of fiber parameters such as dispersion, nonlinearity, zero dispersion wavelength, single mode threshold, etc., The optical characteristics such as dispersion, nonlinearity has been studied for defect core PCF and compared with conventional silica counterpart. Different geometries of PCF with a wide range of air hole and defect size are considered, and the role of defect size in the fiber characteristics was highlighted. To ensure single mode operation, we also evaluated the  $V_{PCF}$  of the designed fibers, which implies that  $V_{PCF}$  decrease with defective air hole radius. Through rigorous numerical analysis, we identified that it is possible to design fiber with a simultaneous increase in nonlinearity along with a minimum positive in the proximity of zero dispersion point. This combination of dispersion and nonlinear profile is identified to be a suitable candidate for nonlinear applications especially SCG.

The second phase of the investigation is dedicated to SCG, where we emphasize the role of defect size in the continuum generation. The incorporation of defect in the core significantly broaden the spectrum as a result of the increase in the soliton order. Through soliton fission theory we comprehensively explained the impact of defect size and highlighted the key role of the Raman soliton self-frequency shift in the spectral broadening process. An octave-spanning continuum has been demonstrated in 1 m of defective core PCF with an air hole diameter of  $d=1.2\mu\text{m}$  and defect size of  $r=0.2\mu\text{m}$ . To conclude, we successfully explained a new means to enhance the PCF based broadband supercontinuum sources, which could potentially find practical applications in the ever-growing photonic technologies.

## 6. ACKNOWLEDGEMENT

The authors fondly remember *the late* Prof. K. Porsezian and thank him for the support during his presence.

## REFERENCES

### References

- [1] J. M. Dudley and J. R. Taylor, "Ten years of nonlinear optics in photonic crystal fibre", *Nat. Photonics*, 3(2), (2009) 85.
- [2] J. M. Dudley and S. Coen, "Supercontinuum generation in photonic crystal fiber", *Rev. Mod. Phys.*, 78(4), (2006) 1135.
- [3] J.R. Taylor, Introduction and History, Chapter 1 in the book: J.M. Dudley, J.R. Taylor, *Optical Fiber Supercontinuum Generation*, Cambridge University Press, Cambridge, UK, 2010.
- [4] J. K. Ranka, R. S. Windeler, and A. J. Stentz, Visible continuum generation in air silica microstructure optical fibers with anomalous dispersion at 800 nm, *Opt. Lett.* 25, (2000), 25.
- [5] J. C. Travers, J. M. Stone, A. B. Rulkov, B. Cumberland, A. K. George, S. V. Popov, J. C. Knight, J. R. Taylor, "Optical pulse compression in dispersion decreasing photonic crystal fiber", *Opt. Exp.*, 15, (2007) 13203.
- [6] Ivan P. Kaminow, Tingye Li, Alan E. Willner, "Optical Fiber Telecommunications", 6th edition, New York: Academic press (2013).
- [7] J. C. Knight, "Photonic Crystal Fibres", *Nature*, 424, (2003) 847.
- [8] R. F. Cregan, B. J. Mangan, J. C. Knight, T. A. Birks, P. S. J. Russell, P. J. Roberts and D. C. Allan, "Single-mode photonic band gap guidance of light in air Science", 285, (1999) 1537.
- [9] J. C. Knight, J. Broeng, T. A. Birks and P. St. J. Russell "Photonic Band Gap Guidance in Optical Fibers", *Science*, 282, (1998) 1476.
- [10] K. M. Ho, C. T. Chan and C. M. Soukoulis, "Existence of a Photonic Gap in Periodic Dielectric Structures", *Physical Review Letters*, 65, (1990) 3152.
- [11] T. A. Birks, J. C. Knight and P. St. J. Russell, "Endlessly Single-Mode Photonic Crystal Fiber", *Optics Letters*, 22, (1997) 961.
- [12] F. Poli, A. Cucinotta, S. Selleri and A. H. Bouk, "Tailoring of flattened dispersion in highly nonlinear photonic crystal fibers", *IEEE Photon. Technol. Lett.*, 16(4), (2004) 1065.
- [13] M. Chen, S.G. Yang, F. F. Yin, H. W. Chen and S. Z. Xie, "Design of a New Type High Birefringence Photonic Crystal Fiber", *Optoelectronics Letters*, 4, (2008) 19.
- [14] K. Saitoh and M. Koshiba, "Chromatic dispersion control in photonic crystal fibers: application to ultra-flattened dispersion", *Opt. Express*, 11, (2003) 843.
- [15] A. Bozolan, C. J. S. de Matos, C. M. B. Cordeiro, E. M. dos Santos, and J. Travers, "Supercontinuum generation in a water-core photonic crystal fiber", *Opt. Exp.*, 16, (2008) 9671.
- [16] G. Fanjoux, S. Margueron, J-C. Beugnot, and T. Sylvestre, "Supercontinuum generation by stimulated RamanKerr scattering in a liquid-core optical fiber", *J. Opt. Soc. Am. B*, 34, (2017) 1677.
- [17] S. E. Kim, B. H. Kim, C. G. Lee, S. Lee, K. Oh and Chul-Sik Kee, "Elliptical defected core photonic crystal fiber with high birefringence and negative flattened dispersion", *Opt. Express*, 20, (2012) 1385.
- [18] B. Kibler, P. A. Lacourt, F. Courvoisier, and J. M. Dudley, "Soliton spectral tunnelling in photonic crystal fibre with subwavelength core defect", *Electron. Lett.*, 43(18), (2007) 967.
- [19] E. E. Serebryannikov and A. M. Zheltikov, "Nanomanagement of dispersion, nonlinearity, and gain of photonic-crystal fibers: qualitative arguments of the Gaussian-mode theory and nonperturbative numerical analysis", *J. Opt. Soc. Am. B*, 23(8), (2006) 1700.
- [20] A. Sharafali, K. Nithyanandan and K. Porsezian, "Self-similar pulse compression by defective core photonic crystal fiber with cubicquintic nonlinearities", *Optik*, 178, (2019) 591.
- [21] W. J. Wadsworth, A. Ortigosa-Blanch, J. C. Knight, T. A. Birks, T. P. M. Man and P. St. J. Russell, "Supercontinuum generation in photonic crystal fibers and optical fiber tapers: a novel light source", *J. Opt. Soc. Am. B*, 19(9), (2002) 2148.
- [22] G. Genty, S. Coen, and J. M. Dudley, "Fiber supercontinuum sources (Invited)", *J. Opt. Soc. Am. B*, 24(8), (2007) 1771.

- [23] G.P.Agrawal, "Nonlinear fiber optics: its history and recent progress [Invited]", *J. Opt. Soc. Am. B*, 28(12), (2011) A1.
- [24] R. R. Alfano, "The Supercontinuum Laser Source-Fundamental with Updated References", 2nd ed. New York: Springer(2006).
- [25] A. Demircan and U. Bandelow, "Analysis of the interplay between soliton fission and modulation instability in supercontinuum generation", *Appl. Phys. B*, 86, (2007) 31.
- [26] M. Nisoli, S. D. Silvetri, O. Svelto, R. Szipcs, K. Ferencz, C. Spielmann, S. Sartania and F. Krausz, "Compression of high-energy laser pulses below 5 fs", *Opt. Lett.*, 22(8), (1997) 522.
- [27] T. Udem, R. Holzwarth and T.W. Hnsch, "Optical frequency metrology", *Nature*, 416, (2002) 233.
- [28] I. Hartl, X. D. Li, C. Chudoba, R. K. Ghanta, T. H. Ko, J.G. Fujimoto, J. K. Ranka and R. S. Windeler, "Ultra-high-resolution optical coherence tomography using continuum generation in an airsilica microstructure optical fiber", *Opt. Lett.* 26, (2001) 608.
- [29] K. Nithyanandan, R. Vasantha Jayakantha Raja, K. Porsezian and T. Uthayakumar, "A colloquium on the influence of versatile class of saturable nonlinear responses in the instability induced supercontinuum generation", *J. Opt. Fib. Tech.*, 19(4), (2013) 348.
- [30] Michael H. Frosz, Ole Bang, and Anders Bjarklev, "Soliton collision and Raman gain regimes in continuous-wave pumped supercontinuum generation", *Opt. Exp.* 14, (2006) 9391.
- [31] RVJ Raja, K Porsezian, K Nithyanandan, "Modulational-instability-induced supercontinuum generation with saturable nonlinear response", *Physical Review A* **82**, (2010) 013825.
- [32] K Nithyanandan, RVJ Raja, K Porsezian, "Power play in the supercontinuum spectra of saturable nonlinear media", *Laser Physics* **24**, (2014) 045405.
- [33] Gil Fanjoux, Samuel Margueron, Jean-Charles Beugnot, and Thibaut Sylvestre, "Supercontinuum generation by stimulated RamanKerr scattering in a liquid-core optical fiber," *J. Opt. Soc. Am. B* 34, (2017) 1677.
- [34] Tianye Huang, Pan Huang, Zhuo Cheng, Jianfei Liao, Xu Wu, Jianxing Pan, "Design and analysis of a hexagonal tellurite photonic crystal fiber with broadband ultra-flattened dispersion in mid-IR", *Optik*, 167 (2018) 144.
- [35] Ajay Kumar Vyas, Elliptical air holes based photonic crystal fiber for narrow band gap and peak power at 1.55 micrometre wavelength, *Optik* **184** (2019) 28.
- [36] Qiang Liu, Qingyu Liu, Yudan Sun, Wei Liu, Chao Liu, Qian Li, Tingting Lv, Tao Sun, Paul K. Chu, "A high-birefringent photonic quasi-crystal fiber with two elliptical air holes", *Optik* **184** 10.
- [37] Hesham Sakr, Rasha A. Hussein, Mohamed Farhat O. Hameed, S.S.A. Obayya, "Analysis of photonic crystal fiber with silicon core for efficient supercontinuum generation, *Optik* **182** (2019) 848.
- [38] Sumaiya Kabir, S. M. Abdur Razzak, "Bending resistive improved effective mode area fluorine doped quadrilateral shaped core photonic crystal fiber for high power fiber lasers, *Optik* **162** (2018) 206.
- [39] Pooja Chauhan, Ajeet Kumar, Yogita Kalra, "A dispersion engineered silica-based photonic crystal fiber for supercontinuum generation in near-infrared wavelength region, *Optik*, **187** (2019) 230.
- [40] Pooja Chauhan, Ajeet Kumar, Yogita Kalra, "Computational modeling of tellurite based photonic crystal fiber for infrared supercontinuum generation, *Optik* **187** (2019) 92.
- [41] Hesham Sakr, Rasha A. Hussein, Mohamed Farhat O. Hameed, S.S.A. Obayya, "Analysis of photonic crystal fiber with silicon core for efficient supercontinuum generation" *Optik* **182** (2019) 848.
- [42] Mohamed Lamine Ferhat, Lynda Cherbi, Issam Haddouche, "Supercontinuum generation in silica photonic crystal fiber at 1.3  $\mu\text{m}$  and 1.65  $\mu\text{m}$  wavelengths for optical coherence tomography, *Optik* **152** (2018) 106.
- [43] K. Porsezian, V.C. Kuriakose (Eds.), *Optical Solitons: Theoretical and Experimental Challenges*, Springer Science Business Media, 2003.
- [44] K. Porsezian, R. Ganapathy (Eds.), *Odyssey of Light in Nonlinear Optical Fibers: Theory and Applications*, CRC Press, Taylor Francis, 2015.
- [45] V.N. Serkin, T.L. Belyaeva, Optimal control for soliton breathers of the Lakshmanan-Porsezian-Daniel, Hirota, and cmKdV models, *Optik - International Journal for Light and Electron Optics* 175 (2018) 17-27.
- [46] F. Li, Q. Li, J. Yuan and P. K. A. Wai, "Highly coherent supercontinuum generation with picosecond pulses by using self-similar compression", *Optic exp.*, 22, (2014) 27339.
- [47] D. Ghosh, S. Bose, S. Roy and S. K. Bhadra, "Design and fabrication of microstructured optical fibers With optimized core suspension for enhanced supercontinuum generation", *J. Lightwave Technol.*, 33, (2015) 4156.
- [48] L. C. Van, A. Anuszkiewicz, A. Ramaniuk, R. Kasztelanic, K. D. Xuan, V. C. Long, M. Trippenbach and R. Buczycki, "Supercontinuum generation in photonic crystal fibres with core filled with toluene", *J. Opt.*, 19, (2017) 125604.
- [49] R. Zhang, J. Teipel and H. Giessen, "Theoretical design of a liquid-core photonic crystal fiber for supercontinuum generation", *Opt. Exp.*, 14, (2006) 6800.
- [50] T. J. Bridges, A. R. Chraplyvy, J. G. Bergman and R. M. Hart, "Broadband infrared generation in liquid-bromine-core optical fibers", *Opt. Lett.*, 7, (1982) 566.
- [51] S. Kedenburg, T. Gissibl, T. Steinle, A. Steinmann, and H. Giessen, "Towards integration of a liquid-filled fiber capillary for supercontinuum generation in the 1.22-4 $\mu\text{m}$  range", *Opt. Express*, 23, (2015) 8281.
- [52] S. Guo, F. Wu, S. Albin, H. Tai and R. S. Rogowski, "Loss and dispersion analysis of microstructured fibers by finite-difference method", *Opt. Exp.*, 12, (2004) 3341.
- [53] G. Ghosh, M. Endo, T. Iwasaki, "Temperature-dependent Sellmeier coefficients and chromatic dispersions for some optical fiber glasses", *J. Light. Tech.*, 12, (1994) 1338.
- [54] S. Couris, M. Renard, O. Faucher, B. Lavorel, R. Chaux, E. Koudoumas and X. Michaut, "An experimental investigation of the nonlinear refractive index ( $n_2$ ) of carbon disulfide and toluene by spectral shearing interferometry and z-scan techniques", *Chem. Phys. Lett.*, 369, (2003) 318.
- [55] T. D. Visser, H. Blok, B. Demeulenaere and D. Lenstra, "Confinement Factors and Gain in Optical Amplifiers", *J. Quantum Electron.*, 33(10), (1997) 1763.
- [56] M. J. Uddin and M. S. Alam, "Dispersion and Confinement Loss of Photonic Crystal Fiber", *Asian Journal of Information Technology*, 7, (2008) 344.
- [57] M. D. Nielsen and N. A. Mortensen, "Photonic crystal fiber design based on the V-parameter", *Opt. Express.*, 11, (2003) 2762.
- [58] J. R. Folkenberg, N. A. Mortensen, K. P. Hansen, T. P. Hansen, H. R. Simonsen, and C. Jakobsen, "Experimental investigation of cut-off phenomena in non-linear photonic crystal fibers", *Opt. Lett.*, 28, (2003) 1882.
- [59] G. P. Agrawal, "Nonlinear Fiber Optics", 5th edition, New York: Academic press (2013).
- [60] R. H. Stolen, J. P. Gordon, W. J. Tomlinson, and H. A. Haus, "Raman response function of silica-core fibers", **6**, (1989) 1159.
- [61] K. J. Blow and D. Wood, "Theoretical Description of Transient Stimulated Raman Scattering in Optical Fibers", *IEEE Journal of Quantum Electron.*, **25**, (1989) 2665.
- [62] V. V. Afanasyev, V. A. Vysloukh, and V. N. Serkin, "Decay and interaction of femtosecond optical solitons induced by the Raman self-scattering effect", *Optics Letters* **15**, (1990) 489.
- [63] E.M. Dianov, A.B. Grudinin, A.M. Prokhorov, V.N. Serkin, "Non-linear transformation of laser radiation and generation of Raman solitons in optical fibers, pages 197-265 in J.R. Taylor (Ed.) *Optical Solitons - Theory and Experiment*, Cambridge Univ, 1992.
- [64] E.M. Dianov, A.Y. Karasik, P.V. Mamyshev, A.M. Prokhorov, V.N. Serkin, M.F. Stelmakh, A.A. Fomichev, Stimulated-Raman conversion of multisoliton pulses in quartz optical fibers, *JETP Lett.* **41** (1985) 294.
- [65] F.M. Mitschke, L.F. Mollenauer, Discovery of the soliton self-frequency shift, *Opt. Lett.* **11** (1986) 659.
- [66] V. N. Serkin, V. A. Vysloukh, J. R. Taylor, "Soliton spectral tunnelling effect", *Electronics Letters* 29, (1993) 12.